

Kinetic and Equilibria Studies of the Aquation of the Trinuclear Platinum Phase II Anticancer Agent $[\{trans\text{-PtCl}(\text{NH}_3)_2\}_2\{\mu\text{-trans-Pt}(\text{NH}_3)_2(\text{NH}_2(\text{CH}_2)_6\text{NH}_2)_2\}]^{4+}$ (BBR3464)

Murray S. Davies,[†] Donald S. Thomas,[†] Alexander Hegmans,[‡] Susan J. Berners-Price,^{*†} and Nicholas Farrell^{*‡}

Departments of Chemistry, University of Western Australia, Crawley WA, 6009, Australia, and Virginia Commonwealth University, Richmond, Virginia 23284-2006

Received August 6, 2001

The hydrolysis profile of the bifunctional trinuclear phase II clinical agent $[\{trans\text{-PtCl}(\text{NH}_3)_2\}_2\{\mu\text{-trans-Pt}(\text{NH}_3)_2(\text{NH}_2(\text{CH}_2)_6\text{NH}_2)_2\}]^{4+}$ (BBR3464, **1**) has been examined using $[\text{H},^{15}\text{N}]$ heteronuclear single quantum coherence (HSQC) 2D NMR spectroscopy. Reported are estimates of the rate and equilibrium constants for the first and second aquation steps, together with the acid dissociation constant ($\text{p}K_{\text{a}1} \approx \text{p}K_{\text{a}2} \approx \text{p}K_{\text{a}3}$). The equilibrium constants for the aquation determined by NMR at 298 and 310 K ($I = 0.1$ M, pH 5.3) are similar, $\text{p}K_1 = \text{p}K_2 = 3.35 \pm 0.04$ and 3.42 ± 0.04 , respectively. At lower ionic strength ($I = 0.015$ M, pH 5.3) the values at 288, 293, and 298 K are $\text{p}K_1 = \text{p}K_2 = 3.63 \pm 0.05$. This indicates that the equilibrium is not strongly ionic strength or temperature dependent. The aquation and anation rate constants for the two-step aquation model at 298 K in 0.1 M NaClO_4 (pH 5.3) are $k_1 = (7.1 \pm 0.2) \times 10^{-5} \text{ s}^{-1}$, $k_{-1} = 0.158 \pm 0.013 \text{ M}^{-1} \text{ s}^{-1}$, $k_2 = (7.1 \pm 1.5) \times 10^{-5} \text{ s}^{-1}$, and $k_{-2} = 0.16 \pm 0.05 \text{ M}^{-1} \text{ s}^{-1}$. The rate constants in both directions increase 2-fold with an increase in temperature of 5 K, and rate constants increase with a decrease in solution ionic strength. A $\text{p}K_{\text{a}}$ value of 5.62 ± 0.04 was determined for the diaqua species $[\{trans\text{-Pt}(\text{NH}_3)_2(\text{OH}_2)\}_2\{\mu\text{-trans-Pt}(\text{NH}_3)_2(\text{NH}_2(\text{CH}_2)_6\text{NH}_2)_2\}]^{6+}$ (**3**). The speciation profile of **1** under physiological conditions is explored and suggests that the dichloro form predominates. The aquation of **1** in 15 mM phosphate was also examined. No slowing of the initial aquation was observed, but reversible reaction between aquated species and phosphate does occur.

Introduction

The complex $[\{trans\text{-PtCl}(\text{NH}_3)_2\}_2\{\mu\text{-trans-Pt}(\text{NH}_3)_2(\text{NH}_2(\text{CH}_2)_6\text{NH}_2)_2\}]^{4+}$ (BBR3464, **1**) is a trinuclear platinum anticancer agent currently in phase II clinical trials.^{1–3} Its development arose from the hypothesis that complexes with

structures significantly different from the archetypal Pt anticancer compound cisplatin would exhibit novel DNA binding and antitumor properties.^{4–9} The flexibility of the hexanediamine linker groups of **1** enables a large number of DNA adducts to be formed, including long-range intra- and interstrand cross-links.^{10–12} The positive charge of **1**, as

* To whom correspondence should be addressed. S.J.B.-P.: phone, +61-8-9380-3258; Fax, +61-8-9380-1005; e-mail, S.Berners-Price@chem.uwa.edu.au. N.F.: phone, 804-828-6320; Fax, 804-828-8599; e-mail, nfarrell@saturn.vcu.edu.

[†] University of Western Australia.

[‡] Virginia Commonwealth University.

- (1) Pratesi, G.; Perego, P.; Polizzi, D.; Righetti, S. C.; Supino, R.; Caserini, C.; Manzotti, C.; Giuliani, F. C.; Pezzoni, G.; Tognella, S.; Spinelli, S.; Farrell, N.; Zunino, F. *Br. J. Cancer* **1999**, *80*, 1912–1919.
- (2) Perego, P.; Caserini, C.; Gatti, L.; Carenini, N.; Romanelli, S.; Supino, R.; Colangelo, D.; Viano, I.; Leone, R.; Spinelli, S.; Pezzoni, G.; Manzotti, C.; Farrell, N.; Zunino, F. *Mol. Pharmacol.* **1999**, *55*, 528–534.
- (3) Calvert, P. M.; Highley, M. S.; Hughes, A. N.; Plummer, E. R.; Azzabi, A. S. T.; Verrill, M. W.; Camboni, M. G.; Verdi, E.; Bernareggi, A.; Zucchetti, M.; Robinson, A. M.; Carmichael, J.; Calvert, A. H. *Clin. Cancer Res.* **1999**, *5*, 3796s.

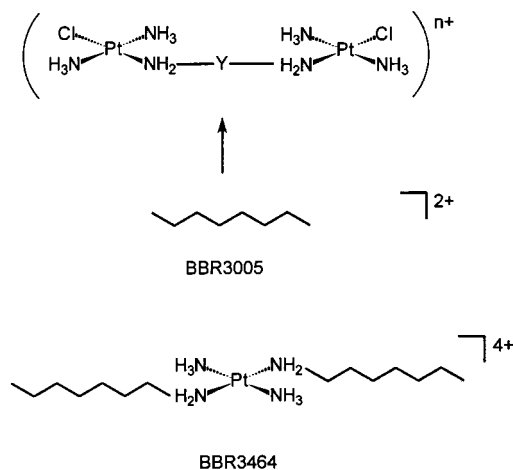
- (4) Farrell, N. In *Advances in DNA Sequence Specific Agents*; Hurley, L. H., Chaires, J. B., Eds.; JAI Press Inc.: Greenwich, CT, 1996; Vol. 2, pp 187–216.
- (5) Farrell, N. *Comm. Inorg. Chem.* **1995**, *16*, 373–389.
- (6) Farrell, N.; Qu, Y.; Hacker, M. P. *J. Med. Chem.* **1990**, *33*, 2179–2184.
- (7) Kraker, A. J.; Hoeschele, J. D.; Elliott, W. L.; Showalter, H. D. H.; Sercel, A. D.; Farrell, N. *J. Med. Chem.* **1992**, *35*, 4526–4532.
- (8) Farrell, N.; Appleton, T. G.; Qu, Y.; Roberts, J. D.; Soares Fontes, A. P.; Skov, K. A.; Wu, P.; Zou, Y. *Biochemistry* **1995**, *34*, 15480–15486.
- (9) Farrell, N.; Qu, Y.; Bierbach, U.; Valsecchi, M.; Menta, E. In *Cisplatin: Chemistry and Biochemistry of a Leading Anticancer Drug*; Lippert, B., Ed.; VCHA, Wiley-VCH: Zurich, 1999; pp 479–496.
- (10) Zehmulová, J.; Kašpárková, J.; Farrell, N.; Brabec, V. *J. Biol. Chem.* **2001**, *276*, 22191–22199.

well as its am(m)ine groups, is believed to facilitate the specific recognition of target sites on DNA through electrostatic and hydrogen-bonding interactions.^{11,12}

It is important to identify the probable hydrolytes and other platinum species that interact and/or react with DNA. The *in vivo* efficacy of any drug is dictated by the balance between metabolic and detoxifying events leading to toxic side effects and the efficiency of target (DNA) interactions. The examination of the aquation of di- and trinuclear Pt complexes is necessary therefore to understand the speciation of the drug and the chemical factors involved in biodistribution. [¹H,¹⁵N] HSQC NMR spectroscopy is a powerful tool for investigating reactions of platinum am(m)ine complexes and has been used to study the aquation of cisplatin^{13,14} and its reactions with DNA sequences with specific binding sites.^{14–17} Sadler et al. have applied it to examine aquation and DNA binding of [PtCl(dien)]⁺,^{18,19} *cis*-[PtCl₂(NH₃)(2-picoline)],^{20,21} and *cis*-[PtCl₂(NH₃)(cyclohexylamine)].^{22,23} We have now begun to apply this technique to di- and trinuclear platinum complexes where complete ¹⁵N-labeling allows observation of all platinated species at micromolar concentrations. The rates of aquation and equilibrium constants of the prototype dinuclear Pt complex, [{*trans*-PtCl(NH₃)₂]₂(μ-NH₂(CH₂)₆NH₂)]²⁺ (1,1/t,t (*n* = 6), BBR3005), were studied and the acid dissociation constants of coordinated aqua ligands of the aquated species determined.²⁴ Most recently we applied [¹H,¹⁵N] HSQC NMR to investigate the mechanism and rates of reaction of 1,1/t,t (*n* = 6) and a 12 base pair duplex oligonucleotide designed such that a 1,4-interstrand cross-link would preferentially form between appropriately positioned guanine bases.²⁵

Dinuclear and trinuclear compounds present a broad range of possible structures incorporating possible bifunctional to tetrafunctional DNA binding modes.^{26,27} The subclass of

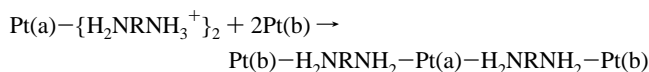
Scheme 1



current interest is best represented by the generic structure depicted in Scheme 1. Surprisingly, incorporation of charge into the linking backbone, through incorporation of either a noncovalent platinum center, as in BBR3464, or a linear polyamine such as spermidine or spermine, actually results in significantly increased cytotoxic and antitumor potency in comparison to “simple” alkanediamine-bridged dinuclear compounds.^{28,29} In mechanistic studies using [¹H,¹⁵N] HSQC NMR our general strategy has been to understand the dinuclear system first. Study and comparison of the trinuclear system then allows delineation of specific contributions of the central charged moiety in metabolic and target interactions. This paper describes the investigation of the aquation profile of [{*trans*-PtCl(¹⁵NH₃)₂]₂{μ-*trans*-Pt(¹⁵NH₃)₂(¹⁵NH₂(CH₂)₆NH₂)₂}]⁴⁺, (BBR3464, **1**, Scheme 1). Reported are the rate and equilibrium constants of the aquation under different conditions of temperature and solution ionic strength, and under the same conditions as those used for reactions between **1** and DNA.³⁰ The acid dissociation constant of the coordinated aqua ligands of [{*trans*-Pt(¹⁵NH₃)₂(OH₂)]₂{μ-*trans*-Pt(¹⁵NH₃)₂(¹⁵NH₂(CH₂)₆NH₂)₂}]⁶⁺ (**3**) (*pK*_{a1} ~ *pK*_{a2} ~ *pK*_{a3}) in 100 mM NaClO₄ is reported, and finally the aquation reaction at 298 K in 15 mM sodium phosphate (pH 5.3) is described.

Experimental Section

Preparation of [{*trans*-PtCl(¹⁵NH₃)₂]₂{μ-*trans*-Pt(¹⁵NH₃)₂(¹⁵NH₂(CH₂)₆NH₂)₂}]⁴⁺ (¹⁵N-**1**). The preparation of the fully ¹⁵N labeled **1** is described elsewhere.³¹ The general strategy for synthesis of trinuclear complexes^{31,32} allows for selective labeling. In brief:



- (11) Brabec, V.; Kašparková, J.; Vraná, O.; Nováková, O.; Cox, J. W.; Qu, Y.; Farrell, N. *Biochemistry* **1999**, *38*, 6781–6790.
- (12) Kloster, M. B. G.; Hannis, J. C.; Muddiman, D. C.; Farrell, N. *Biochemistry* **1999**, *38*, 14731–14737.
- (13) Berners-Price, S. J.; Frenkiel, T. A.; Frey, U.; Ranford, J. D.; Sadler, P. J. *J. Chem. Soc., Chem. Commun.* **1992**, 789–791.
- (14) Davies, M. S.; Berners-Price, S. J.; Hambley, T. W. *Inorg. Chem.* **2000**, *39*, 5603–5613.
- (15) Berners-Price, S. J.; Barnham, K. J.; Frey, U.; Sadler, P. J. *Chem.—Eur. J.* **1996**, *2*, 1283–1291.
- (16) Davies, M. S.; Berners-Price, S. J.; Hambley, T. W. *J. Am. Chem. Soc.* **1998**, *120*, 11380–11390.
- (17) Davies, M. S.; Berners-Price, S. J.; Hambley, T. W. *J. Inorg. Biochem.* **2000**, *79*, 167–172.
- (18) Guo, Z.; Chen, Y.; Zang, E.; Sadler, P. J. *J. Chem. Soc., Dalton Trans.* **1997**, 4107–4111.
- (19) Murdoch, P. del S.; Guo, Z.; Parkinson, J. A.; Sadler, P. J. *J. Biol. Inorg. Chem.* **1999**, *4*, 32–38.
- (20) Chen, Y.; Guo, Z.; Parsons, S.; Sadler, P. J. *Chem.—Eur. J.* **1998**, *4*, 672–676.
- (21) Chen, Y.; Parkinson, J. A.; Guo, Z.; Brown, T.; Sadler, P. J. *Angew. Chem., Int. Ed.* **1999**, *38*, 2060–2063.
- (22) Barton, S. J.; Barnham, K. J.; Habtemariam, A.; Sue, R. E.; Sadler, P. J. *Inorg. Chim. Acta* **1998**, *273*, 8–13.
- (23) Barton, S. J.; Barnham, K. J.; Frey, U.; Habtemariam, A.; Sue, R. E.; Sadler, P. J. *Aust. J. Chem.* **1999**, *52*, 173–177.
- (24) Davies, M. S.; Cox, J. W.; Berners-Price, S. J.; Barklage, W.; Qu, Y.; Farrell, N. *Inorg. Chem.* **2000**, *39*, 1710–1715.
- (25) Cox, J. W.; Berners-Price, S. J.; Davies, M. S.; Farrell, N.; Qu, Y. *J. Am. Chem. Soc.* **2001**, *123*, 1316–1326.
- (26) Farrell, N.; Qu, Y.; Roberts, J. D. In *Topics in Biological Inorganic Chemistry*; Clarke, M. J., Sadler, P. J., Eds.; Springer-Verlag: New York, 1999; pp 99–115.

- (27) Qu, Y.; Rauter, H.; Fontes, A. P. S.; Bandarage, R.; Kelland, L. R.; Farrell, N. *J. Med. Chem.* **2000**, *43*, 3189–3192.
- (28) Farrell, N. In *Platinum Based Drugs in Cancer Chemotherapy*; Kelland, L. R., Farrell, N., Eds.; Humana Press: Totawa, NJ, 2000; pp 321–338.
- (29) Rauter, H.; Di Domenico, R.; Menta, E.; Oliva, A.; Qu, Y.; Farrell, N. *Inorg. Chem.* **1997**, *36*, 3919–3927.
- (30) Berners-Price, S. J.; Davies, M. S.; Thomas, D. S.; Hegmans, A.; Farrell, N. Unpublished results.

In the specific case of **1** (BBR3464), the Pt(a) moiety is derived from reaction of linking 1,6-hexanediamine with *trans*-[PtCl₂(NH₃)₂]. Coupling of this central unit with further *trans*-[PtCl₂(NH₃)₂] as Pt(b) gives the desired species. The opportunities for selective ¹⁵N labeling are evident. The form in which all NH₃ and NH₂ groups in the complex are ¹⁵N labeled is designated “fully labeled”, while “end labeled” describes **1** in which only the NH₃ groups on the terminal Pt atoms are ¹⁵N labeled.

NMR Spectroscopy. The NMR spectra were recorded on a Varian UNITY-INOVA-600 MHz spectrometer (¹H, 599.92 MHz; ¹⁵N, 60.79 MHz). The ¹H NMR chemical shifts were internally referenced to 1,4-dioxane (δ 3.767) and the ¹⁵N chemical shifts externally referenced to ¹⁵NH₄Cl (1.0 M in 1.0 M HCl in 5% D₂O in H₂O). The two-dimensional [¹H,¹⁵N] heteronuclear single-quantum coherence (HSQC) NMR spectra (decoupled by irradiation with the GARP-1 sequence during the acquisition) were recorded using the sequence of Stonehouse et al.³³ and processed as described previously.¹⁶ Concentrations of species were determined by integration of the two-dimensional cross peaks using the Varian VNMR software and normalization of the peak volumes and then conversion to concentration based on their relative volume and the initial concentration of **1**.

pH Measurements. For the pK_a determination the pH was measured using a Corning pH Micro NMR Combo electrode (476486) and an Ecoscan pH meter. For the kinetics experiments the pH values were determined using a Shindengen pH Boy-P2 (su19A) pH meter. To avoid leaching of chloride, aliquots of 5 μ L of the solution were placed on the electrode and the pH was recorded (the aliquots were not returned to the sample). Both meters were calibrated using pH buffers at pH 6.9 and 4.0. Adjustments in pH were made using 0.1 and 0.01 M HClO₄, or 0.1 and 0.01 M NaOH.

Aquation Experiments. Sample Preparation. (i) 100 mM NaClO₄. A solution of fully ¹⁵N labeled **1** (3.34 mg, 2.67 μ mol) was prepared in 650 μ L of 5% D₂O/95% H₂O (100 mM NaClO₄) to give a concentration of 4.11 mM. The sample was incubated at 310 K for 24 h, and then at 298 K for a further 24 h. [¹H,¹⁵N] HSQC NMR spectra were recorded at each temperature. The final solution pH was 5.1.

The kinetics of the aquation reaction were studied on a freshly prepared sample of fully ¹⁵N labeled **1** (2.04 mg, 1.63 μ mol) in 100 mM NaClO₄ in 5% D₂O/95% H₂O (400 μ L) to give a concentration of 4.08 mM. [¹H,¹⁵N] NMR spectra were recorded at 298 K over a period of 6 h. The pH of the solution was monitored from the ¹H/¹⁵N chemical shifts of the aquated species (Figure 4) and decreased from ca. 4.8 to 4.5 over the course of the reaction.

(ii) 15 mM ClO₄⁻ or PO₄³⁻. Solutions were prepared by dissolving end ¹⁵N labeled **1** (1.90–2.22 mg, 1.53–1.79 μ mol) in 15 mM NaClO₄ (pH 5.3) in 5% D₂O/95% H₂O (454–527.5 μ L) or 15 mM sodium phosphate buffer (pH 5.3) in 5% D₂O/95% H₂O (451.5 μ L) to give initial concentrations of ¹⁵N-**1** of 3.39 mM. After sonication for 1 min the samples were transferred to NMR tubes and placed in the NMR spectrometer at the desired temperature for the duration of the kinetic experiments (3.25–15.5 h). Experiments were conducted at 288, 293, and 298 K (perchlorate) and 298 K (phosphate). [¹H,¹⁵N] HSQC NMR spectra were recorded

at 15 min intervals until equilibrium conditions were attained. The final pH of the solutions in perchlorate were unchanged (pH = 5.3) while for the phosphate solution the pH decreased to \sim 4.0 over the course of the reaction.

Data Analysis. For the reactions in aqueous perchlorate solution the concentrations of **1**, **2**, and **3** at each time point were calculated from the relative volumes of the ¹H/¹⁵N peaks for **1/2** and **2/3** (see Figure 1), in the same manner as previously applied to 1,1,t ($n = 6$).^{24,34} The correction for peak overlap was carried out in two ways; the first method (model 1) assumed no formation of **3**, and the second method (model 2) assumed that aquation of the second chloro ligand from **2** was equally probable as aquation of the first chloro ligand from **1** so that the ratio of the concentrations of **1:2** is equal to **2:3** at each time point. According to this model, the more intense peak (δ 3.84/–64.7) is derived from the total concentration of **1** plus 50% of **2**, and the minor peak ($\delta \sim$ 4.10/–61.9) the total concentration of **3** plus 50% of **2**. The rationale behind this treatment is that the two positively charged {PtN₃} groups are separated by two six carbon chain linkers and the central PtN₄ linker, a distance of \sim 25 Å. At this distance, one {PtN₃} group should not be affected by the environment of the other,²⁴ and each end can be treated as an independent entity. In the aquation studies, both the rate and equilibrium constants have assumed that all the aquated species is in the aqua form, and that none is in the hydroxo form. In the pH range (<5.4) at which the experiments were undertaken >70% is in the aqua form, on the basis of the pK_a of the aquated aqua ligand (5.62) (see below). The kinetic model for the aquation in phosphate solution assumed that no formation of **3** occurred, but included a chlorophosphato species **7** and a aqua-phosphato species **8**. The kinetic models for all these reactions are depicted and the rate and equilibrium constants are defined in Scheme 2. The data were fitted to appropriate reversible aquation models using the program SCIENTIST (MicroMath, version 2.01). In all models a 5% initial concentration of Cl/H₂O (**2**) was assumed. This gave superior fits to the kinetic data and may be justified on the basis of the sonication of the sample hastening the aquation process. Copies of representative models together with kinetic plots of all the reactions are provided as Supporting Information.

pK_a determination of [trans-Pt(NH₃)₂(OH)₂]₂{ μ -trans-Pt(NH₃)₂(NH₂(CH₂)₆NH₂)₂]⁶⁺ (3**).** AgNO₃ (188.8 mg, 1.11 mmol) was dissolved in H₂O (1.5 mL), and a 4.3 μ L (1.8 equiv) aliquot was added to an Eppendorf tube charged with fully ¹⁵N labeled **1** (2.29 mg, 1.76 μ mol) and 1,4-dioxane (5 μ L of 13.3 mM in 5% D₂O/95% H₂O). After 24 h protected from light, the mixture was centrifuged and the AgCl precipitate removed. NaClO₄ (18.8 mg, 1.54 mmol) in D₂O (75 μ L) was added to the supernatant, giving concentrations of **3** (1.11 mM) and ClO₄⁻ (97.5 mM). Examination of the [¹H,¹⁵N] HSQC NMR spectrum indicated small amounts (<10%) of the chloro forms **1/2**, but their presence did not compromise the experiment. Adjustments in pH were carried out by addition of NaOH (0.1 or 0.01 M in 5% D₂O/95% H₂O) and HClO₄ (0.1 or 0.01 M in 5% D₂O/95% H₂O), respectively. ¹H and [¹H,¹⁵N] NMR spectra were recorded in the pH range 3.4–8.4.

The pH titration data were analyzed using the equation

$$\delta = (\delta_A[\text{H}^+] + \delta_B K_a)/([\text{H}^+] + K_a) \quad (1)$$

where K_a is the acid dissociation constant for one Pt–OH₂ group

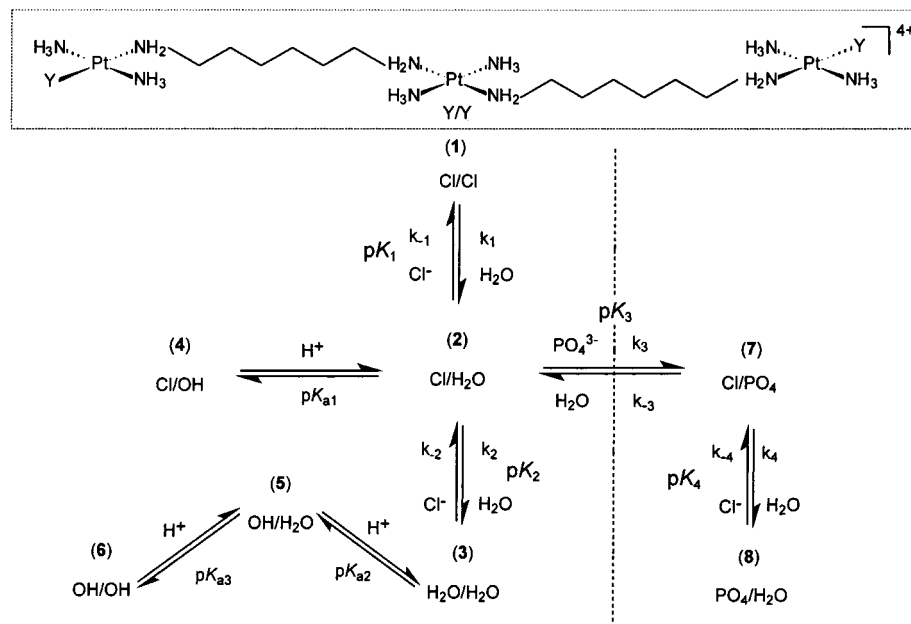
(31) Valsecchi, M.; Menta, E.; Di Domenico, R.; da Re, G.; Lotto, A.; Conti, M.; Spinelli, S.; Bugati, C.; Manzotti, C.; Rauter, H.; Qu, Y.; Farrell, N. Manuscript in preparation.

(32) Qu, Y.; Appleton, T. G.; Hoeschele, J. D.; Farrell, N. *Inorg. Chem.* **1993**, *32*, 2591–2593.

(33) Stonehouse, J.; Shaw, G. L.; Keeler, J.; Laue, E. D. *J. Magn. Reson., Ser. A* **1994**, *107*, 174–184.

(34) For clarity we refer only to the aquated species (**2** and **3**) although at this pH the ¹H,¹⁵N peak represents the weighted average of aqua and hydroxo forms. The ¹H and ¹⁵N shifts of the individual species are derived from the titration curves (Figure 4).

Scheme 2



of the diaqua complex **3** and δ_A and δ_B are the chemical shifts of the diaqua (**3**) and dihydroxo (**6**) complexes, respectively. The program KaleidaGraph (Synergy Software, Reading, PA) was used for fitting.

Results

Two forms of ^{15}N -labeled $[\{trans\text{-PtCl}(\text{NH}_3)_2\}_2(\mu\text{-trans-Pt}(\text{NH}_3)_2(\text{NH}_2(\text{CH}_2)_6\text{NH}_2)_2)]^{4+}$ (**1**) were prepared by the synthetic methods described by Valsecchi et al.³¹ “Fully labeled” describes **1** in which all NH_3 and NH_2 groups in the complex are ^{15}N labeled, while “end labeled” describes **1** in which only the NH_3 groups on the terminal (end) Pt atoms are ^{15}N labeled. The $[\text{H},^{15}\text{N}]$ HSQC NMR spectrum of fully ^{15}N labeled **1** recorded after 24 h at 298 K is shown in Figure 1, and the shifts of the $^{15}\text{NH}_3$ and $^{15}\text{NH}_2$ resonances are listed in Table 1. In both the $^{15}\text{NH}_3$ and $^{15}\text{NH}_2$ regions of the spectrum peaks corresponding to the $\{\text{PtN}_3\text{X}\}$ (end) and $\{\text{PtN}_4\}$ (linker) groups (L) are well-separated. The ^1H and ^{15}N shifts of the linker $\text{Pt}-^{15}\text{NH}_3$ (δ 4.08/−63.8) and $\text{Pt}-^{15}\text{NH}_2$ (δ 4.61/−44.0) groups (labeled L in Figure 1) are insensitive to aquation of the end groups so that no new peaks appear in these regions. The terminal $\text{Pt}-^{15}\text{NH}_3$ and $\text{Pt}-^{15}\text{NH}_2$ groups for **1** have peaks at δ 3.84/−64.7 and 4.97/−46.9, respectively, that are similar to those of 1,1/*t,t* ($n = 6$).²⁴ The aquation is readily followed by the appearance of new peaks in both regions (Figure 1) assignable to the $\{\text{PtON}_3\}$ group of the mono- and diaquated species (**2** and **3**).³⁴ As observed for 1,1/*t,t* ($n = 6$)²⁴ the peaks for the $\{\text{PtClN}_3\}$ group of the monoaquated species are not visible and must be coincident with those of **1**. A shift to high field of the $\text{Pt}-\text{NH}_2$ ^{15}N resonance by ~ 18 ppm is consistent with replacement of the *trans* chloro ligand by the oxygen donor of H_2O .^{35,36} For the $\text{Pt}-\text{NH}_3$ groups the ^{15}N shift is not diagnostic of the nature of the *cis* ligand. Nevertheless

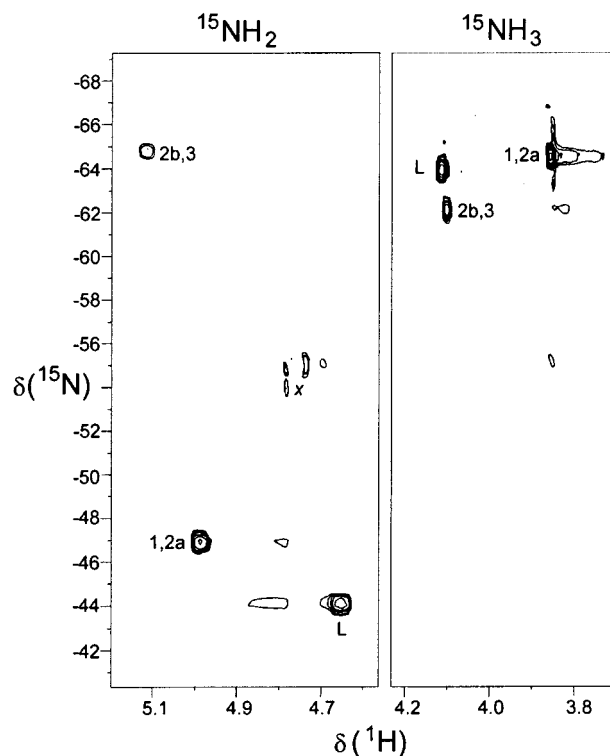


Figure 1. $[\text{H},^{15}\text{N}]$ HSQC NMR spectrum of fully labeled ^{15}N -**1** in 100 mM NaClO_4 (95% $\text{H}_2\text{O}/5\%$ D_2O) (pH 5.3) after 24 h at 298 K. The resonances are assigned to the $\text{Pt}-\text{NH}_3$ and $\text{Pt}-\text{NH}_2$ groups in **1** and the aquachloro species **2** (see Scheme 2). The peaks for **1** are superimposed with one of the two peaks (in each region) for **2**, and the other peaks for **2** are superimposed with those of the diaqua species **3**, but this latter species represents a minor contribution at equilibrium.³⁴ Peaks representing the central PtN_4 grouping are indicated “L”, peaks labeled “*” are ^{195}Pt satellites, and peaks labeled “x” are artifacts.

significant shifts occur in both ^1H and ^{15}N dimensions so that peaks for the aquated species can be distinguished from

(35) Appleton, T. G.; Hall, J. R.; Ralph, S. F. *Inorg. Chem.* **1985**, *24*, 4685–4693.

(36) Qu, Y.; Farrell, N.; Valsecchi, M.; de Greco, L.; Spinelli, S. *Magn. Reson. Chem.* **1993**, *31*, 920–924.

Table 1. ^1H and ^{15}N Chemical Shifts for **1**, the Aqueated Species **3** and **6**,^a and Phosphato Species **7** and **8**^b at 298 K

complex	$^{15}\text{NH}_3^c$		$^{15}\text{NH}_2^c$	
	δ ^1H	δ ^{15}N	δ ^1H	δ ^{15}N
1 (Cl/Cl)	3.84	-64.7	4.97	-46.9
3 ($\text{H}_2\text{O}/\text{H}_2\text{O}$) ^d	4.09	-61.9	5.12	-65.1
6 (OH/OH) ^{d,e}	3.83	-63.0	4.46	-56.9
7a (Cl/ PO_4) ^f	3.84	-64.7		
7b (PO_4 /Cl) ^f	3.93	-61.1		
8a ($\text{H}_2\text{O}/\text{OH}/\text{PO}_4$) ^{f,g}	4.12	-60.8		
8b ($\text{PO}_4/\text{H}_2\text{O}/\text{OH}$) ^{f,g}	3.96	-61.1		

^a 0.1 M NaClO_4 in 95% $\text{H}_2\text{O}/5\%$ D_2O , 298 K. Only the $^1\text{H}/^{15}\text{N}$ shifts of the end Pt-am(m)ine groups are listed; the shifts of the linker group are unaffected by the ligation on the terminal Pt atoms, δ $^1\text{H}/^{15}\text{N} = 4.08/-63.8$, $4.41/-44.0$. ^b 15 mM PO_4^{3-} , pH 5.3, 298 K. ^c ^1H referenced to dioxane at 3.767 ppm; ^{15}N referenced to $^{15}\text{NH}_4\text{Cl}$ (external). ^d Values obtained by fitting eq 1 (Figure 4). ^e Only one inflection point is observed for the pH titration curve of **3**, so species **5** ($\text{OH}/\text{H}_2\text{O}$) and **6** (OH/OH) cannot be discriminated. ^f The reaction was carried out using end-labeled material, so other shifts are unavailable. ^g At pH 5.3 the aqua/hydroxo ligation is a mixture.

the dichloro species **1**. This permitted the use of the end-labeled species to follow the aquation reaction of **1** in 15 mM perchlorate or phosphate solution.

Aquation of 1. Measurement of Pt- $^{15}\text{NH}_3$ $^1\text{H}/^{15}\text{N}$ HSQC NMR peak volumes for a solution of fully ^{15}N labeled **1** in 100 mM NaClO_4 at 310 K for 24 h gave the ratio of peaks (**1/2**):(**2/3**) = $(83.8 \pm 0.6):(16.2 \pm 0.6)$ affording $\text{p}K_1 = 3.20 \pm 0.05$ using the model in which only one chloro group is aquated (model 1) and $\text{p}K_1 = \text{p}K_2 = 3.42 \pm 0.04$ using the model incorporating both aquation steps (model 2) (see Scheme 2).³⁷ When the same solution was equilibrated at 298 K for a further 24 h, the ratio of peaks (**1/2**):(**2/3**) was $(83.4 \pm 0.6):(16.6 \pm 0.6)$ giving equilibrium constants of $\text{p}K_1 = 3.14 \pm 0.04$ (model 1) and $\text{p}K_1 = \text{p}K_2 = 3.35 \pm 0.04$ (model 2). Aquation reactions using end ^{15}N -**1** were also carried out in 15 mM NaClO_4 , at 288, 293, and 298 K. These conditions were chosen to enable direct comparison of the rates of aquation in the absence of DNA with those obtained in DNA binding experiments.³⁰ The [$^1\text{H},^{15}\text{N}$] HSQC NMR spectrum at equilibrium at 298 K is shown as Figure 2a. For each of the three temperatures the ratio of peak volumes (**1/2**):(**2/3**) was similar, $(86.0 \pm 1.0):(14.0 \pm 1.0)$. From these data we obtained the average equilibrium constants $\text{p}K_1 = 3.42 \pm 0.05$ (model 1) and $\text{p}K_1 = \text{p}K_2 = 3.63 \pm 0.05$ (model 2) (see Table 2).

Figure 3 (a and b) shows the time dependence of species present during the aquation of **1** at 298 K in 15 mM perchlorate, where the concentrations of **1**, **2**, **3**, and Cl^- are derived using both aquation models. The concentration of **1** is seen to decrease from its initial value of 3.38 mM to an equilibrium value of approximately 2.5 mM within 2 h. Equilibrium is achieved marginally more slowly in 100 mM

(37) The equilibrium constants $\text{p}K_n$ are not true equilibrium constants because no account has been made of the relative contributions of aqua and hydroxo ligation to the total at the given pH. This is also true for the rate constants. However, in all cases the solution pH is lower by at least 0.3 pH unit than the $\text{p}K_a$ of the coordinated aqua ligand, and so the major form will be the aqua species. As much as possible all experiments were carried out at the same pH, which enables direct comparison between the values obtained at different temperatures and between the two kinetic models.

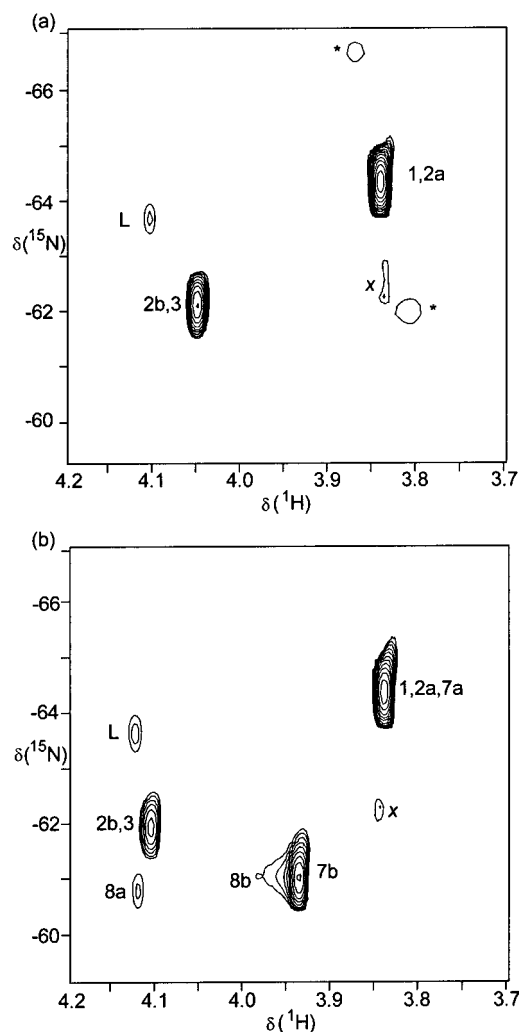


Figure 2. [$^1\text{H},^{15}\text{N}$] HSQC NMR spectra of end-labeled ^{15}N -**1** in (a) 15 mM ClO_4^- (95% $\text{H}_2\text{O}/5\%$ D_2O) (pH 5.3) after 2.9 h and (b) 15 mM PO_4^{3-} (95% $\text{H}_2\text{O}/5\%$ D_2O) (pH 5.3) after 14.3 h at 298 K. Peaks labeled “*” are ^{15}Pt satellites, those labeled “x” are artifacts, and “L” indicates the central PtN_4 grouping which appears because of ^{15}N impurities in the sample. The peak assignments are shown in Scheme 2. On the basis of the position of the peaks, it is likely that peaks **7b** and **8b** correspond to the {PtO-(phosphato) N_3 } groups of **7** and **8**, respectively, and peaks **7a** and **8a** correspond to the {PtCl N_3 } and {PtO(aqua) N_3 } groups of these species, but this has not been confirmed.

ClO_4^- at the same temperature. The derived rate constants for the aquation of **1** under different reaction conditions are listed in Table 2 alongside the corresponding equilibrium constants. Time dependence plots for aquation reactions under the different conditions are provided as Supporting Information. Examination of the rate constants for the aquation of **1** at 288, 293, and 298 K (Table 2) shows that the aquation rate constant k_1 increases with temperature, approximately doubling with an increment of 5 K. The anation rate constant k_1 increases in proportion, such that equilibrium is achieved more rapidly at higher temperature but the position of the equilibrium remains the same. Both the aquation and anation rate constants are higher at lower ionic strengths, resulting in a shift in the equilibrium toward the dichloro form.

Aquation of 1 in the Presence of Phosphate. When the aquation of **1** was carried out in 15 mM phosphate solution,

Table 2. Equilibrium and Rate Constants for the Hydrolysis of **1** (Scheme 2) in Comparison to 1,1/t,t ($n = 6$) in 15 or 100 mM NaClO₄ (pH 5.3)

compound	T (K)	μ (mM)	$pK_1 = pK_2^a$	k_1 (10^{-5} s^{-1})	k_{-1} ($\text{M}^{-1} \text{ s}^{-1}$)	k_2 (10^{-5} s^{-1})	k_{-2} ($\text{M}^{-1} \text{ s}^{-1}$)
1,0,1/t,t,t ($n = 6$) (1) ^a	310	100	3.42 ± 0.04				
	298	100	3.35 ± 0.04	7.1 ± 0.2	0.158 ± 0.013	7.1 ± 1.5	0.16 ± 0.05
	298	15	3.64 ± 0.01	9.2 ± 0.2	0.40 ± 0.01	9.2 ± 0.7	0.40 ± 0.04
	293	15	3.58 ± 0.01	4.77 ± 0.08	0.182 ± 0.004	4.8 ± 0.3	0.18 ± 0.02
	288	15	3.66 ± 0.01	2.58 ± 0.01	0.118 ± 0.003	2.6 ± 0.2	0.12 ± 0.02
1,1/t,t ($n = 6$) ^{b,c}	310	b	4.16 ± 0.02	7.9 ± 0.2	1.18 ± 0.06	7.9 ± 2.6	1.2 ± 0.6

^a Determined using both aquation steps model (model 2). ^b From ref 24, data were obtained from a 2.0 mM solution in H₂O. ^c The values of the equilibrium and rate constants for 1,1/t,t ($n = 6$) were recalculated using model 2 in the same manner as applied here for **1**.

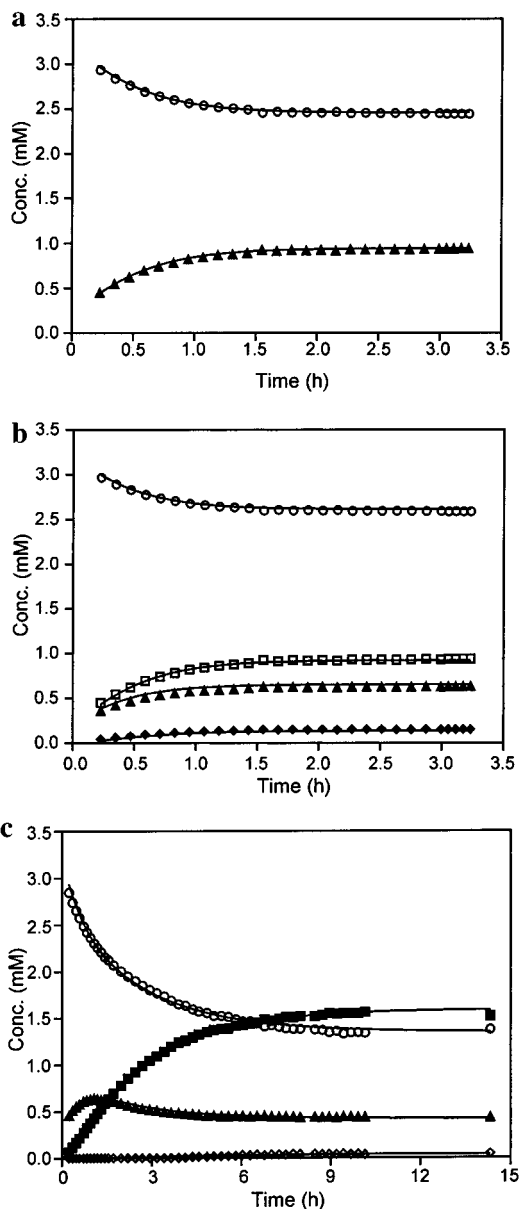


Figure 3. Plots of the time dependence of species in the aquation of ¹⁵N-**1** at 298 K in 15 mM NaClO₄ (95% H₂O/5% D₂O) (pH 5.3) according to (a) the single aquation model (model 1) and (b) both aquation steps model (model 2) and (c) in 15 mM phosphate solution (95% H₂O/5% D₂O) (pH 5.3) at 298 K. Key: **1**, ○; **2**, ▲; **3**, ◆; **7**, ■; **8**, ◇; Cl⁻, □.

additional peaks are seen in the [¹H,¹⁵N] HSQC NMR spectra, indicating that binding of phosphate to the Pt complex is occurring (see Figure 2b). The first [¹H,¹⁵N] spectrum recorded (after 10 min) has an additional ¹H/¹⁵N peak at δ 3.93/−61.1 relative to the spectrum of **1** in aqueous per-

Table 3. Equilibrium and Rate Constants for the Aquation of ¹⁵N-**1** in 15 mM ClO₄⁻ and 15 mM PO₄³⁻ (at pH 5.3, 298 K), According to the Model Shown as Scheme 2^a

parameter	15 mM ClO ₄ ⁻ (298 K) ^b	15 mM PO ₄ ³⁻ (298 K)
k_1 (10^{-5} s^{-1})	10.7 ± 0.1	11.1 ± 0.1
k_{-1} ($\text{M}^{-1} \text{ s}^{-1}$)	0.294 ± 0.004	0.172 ± 0.003
k_3 ($\text{M}^{-1} \text{ s}^{-1}$)		0.0163 ± 0.0002
k_{-3} (10^{-5} s^{-1})		5.72 ± 0.12
k_4 (10^{-5} s^{-1})		0.26 ± 0.10
k_{-4} ($\text{M}^{-1} \text{ s}^{-1}$)		0.05 ± 0.03
pK_1	3.44 ± 0.04	3.19 ± 0.01
pK_3		-2.45 ± 0.01
pK_4		4.3 ± 0.3

^a Using an initial concentration of **1** of 3.38 mM. ^b Data according to the single aquation model, model 1. Data for 288 and 293 K experiments using model 1 are listed as Supporting Information.

chlorate. This peak (**7b** in Figure 2b) eventually becomes more prominent than that of the aquachloro species **2** and is most reasonably attributed to the {PtON₃} unit of the chlorophosphato species (**7**), in which the partner **7a** {PtClN₃} peak is superimposed with that of **1**. Later in the reaction (4 h) a new peak emerges at δ 4.12/−60.8 with a partner peak at δ 3.96/−61.1 that is less clearly defined, due to its close proximity to peak **7b**. These two peaks are assigned to the aquaphosphato species where **8a** and **8b** represent the aqua and phosphato binding, respectively.

The time dependence of the concentrations of species in the presence of PO₄³⁻ and the kinetic fit derived from Scheme 2 are shown in Figure 3c. The initial process of aquation of **1** is the same as that in aqueous perchlorate, with aquation and anation rate constants of similar magnitude (see Table 3). The aquachloro species **2** builds up to a maximum concentration of ~20% of the total platinum species after 1 h and then decreases to an equilibrium concentration of ~15% of the total platinum species. The reaction mechanism (as shown in Scheme 2) has been modeled such that **2** reacts by phosphate displacement of the aqua ligand to form a chlorophosphato species **7**. The direct reaction between **1** and phosphate cannot be ruled out, but for the purposes of the kinetic fit, prior aquation of **1** to form **2** was assumed and the aquation of **2** to **3** was not considered. All processes in the reaction have been treated as reversible, as equilibrium is achieved after approximately 12 h. The concentration of **7** increases to an equilibrium concentration of more than 50% of the total platinum species after approximately 10 h. Aquation of the chloro ligand of **7** to form the aquaphosphato species **8** occurs only to a limited extent.

pK_a Determinations of the Diaqua Adduct **3.** A sample of the aquated form **3** (in 0.1 M NaClO₄) was prepared from

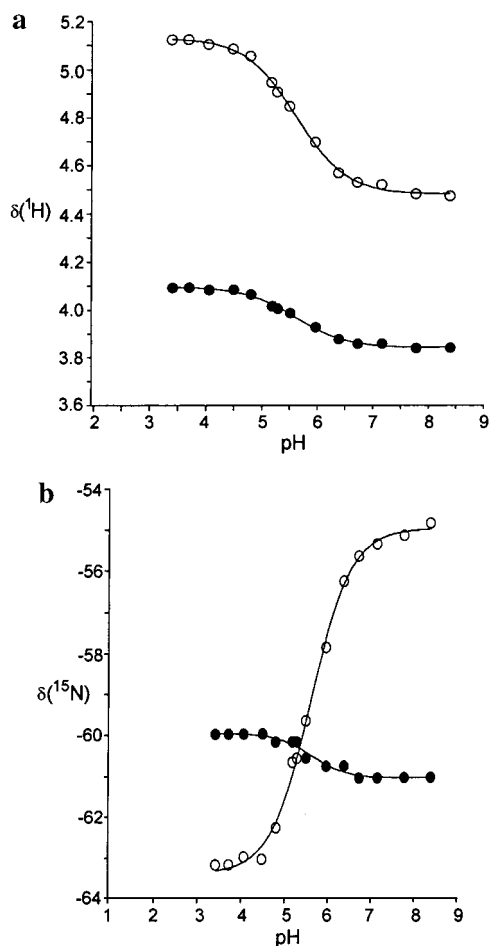


Figure 4. (a) Plot of the ^1H chemical shifts of the $^{15}\text{NH}_3$ (●) and $^{15}\text{NH}_2$ (○) protons of ^{15}N -3 in 100 mM NaClO_4 (95% $\text{H}_2\text{O}/5\%$ D_2O) as a function of pH. The pK_a values obtained are $\delta(^{15}\text{NH}_3)$ 5.62 ± 0.04 , $\delta(^{15}\text{NH}_2)$ 5.63 ± 0.02 . (b) Plot of ^{15}N chemical shifts of the $^{15}\text{NH}_3$ (●) and $^{15}\text{NH}_2$ (○) groups of ^{15}N -3 in 100 mM NaClO_4 (95% $\text{H}_2\text{O}/5\%$ D_2O) as a function of solution pH. The pK_a values obtained are $\delta(^{15}\text{NH}_3)$ 5.64 ± 0.08 , $\delta(^{15}\text{NH}_2)$ 5.63 ± 0.04 .

fully ^{15}N labeled **1** by removal of Cl^- by treatment with Ag^+ . The $[^1\text{H}, ^{15}\text{N}]$ NMR spectrum of the solution at pH 3.4 contained two major peaks at 5.16/−65.3 and 4.11/−62.1 assignable to the $\text{Pt}-\text{NH}_2$ and $\text{Pt}-\text{NH}_3$ groups of **3**. This solution was titrated over the pH range 3.4–8.4, and the pK_a of the aqua/hydroxo ligand(s) was determined by $[^1\text{H}, ^{15}\text{N}]$ NMR by monitoring the pH dependences of the ^1H and ^{15}N shifts of both the $\text{Pt}-^{15}\text{NH}_3$ and $\text{Pt}-^{15}\text{NH}_2$ groups (Figure 4). The chemical shifts of the fully aqua (**3**) or hydroxo species (**6**) are listed in Table 1.

The shifts of the $\text{Pt}-^{15}\text{NH}_2$ group (*trans* to O) are more sensitive to pH than the shifts of the $\text{Pt}-^{15}\text{NH}_3$ groups (*cis* to O) (see Figure 4). The changes in ^1H chemical shift on deprotonation for the $^{15}\text{NH}_2$ ($\Delta\delta$ 0.6) and $^{15}\text{NH}_3$ ($\Delta\delta$ 0.3) groups are in good agreement with those observed previously for 1,1/*t,t* ($n = 6$).²⁴ The four pH titration curves were fitted to eq 1 to give the pK_a values shown in Figure 4. The data derived from the ^{15}N shift of the NH_3 groups have a larger error due to the relatively small change in the chemical shift combined with the low resolution in the ^{15}N dimension (δ ca. ± 0.1 ppm). A pK_a value of 5.62 ± 0.04 was obtained on the basis of ^1H chemical shifts. This result is consistent

with values found by potentiometric methods (data not shown).

Discussion

^{15}N -Labeling of **1** and use of $[^1\text{H}, ^{15}\text{N}]$ HSQC NMR spectroscopy has allowed us to study the speciation profile for this trinuclear phase II clinical agent in aqueous solution. These results now allow us to compare the aquation behavior with that of the dinuclear prototype 1,1/*t,t* ($n = 6$)²⁴ and also with cisplatin and other mononuclear Pt complexes.

The equilibrium constant for the aquation pK_1 (Scheme 2, Table 2) is lower than that of the related dinuclear complex 1,1/*t,t* ($n = 6$),²⁴ under similar conditions (298 K, pH 5.3), indicating that the equilibrium for **1** lies further toward the aquated species. Nevertheless, the equilibrium constants show that the dichloro form of **1** is still strongly favored over the aquated forms, under the conditions used. The equilibrium constant was found to be slightly dependent on the ionic strength of the solution, with lower pK_1 values obtained at higher ionic strength. A similar trend of decreasing pK_1 with increases in solution ionic strength has been found by House and co-workers in studies on the aquation of cisplatin.^{38,39}

There is little difference in the equilibrium constants with a change in solution temperature. In the range 288–298 K the equilibrium constants (under the same ionic strength and pH conditions) are the same within experimental uncertainties. The same behavior was observed with 1,1/*t,t* ($n = 6$)²⁴ and is in marked contrast to that seen for cisplatin,^{38,40,41} where lower pK_1 values are obtained at higher temperatures. Similarly, Coley and Martin⁴² found that for $[\text{PtCl}_2(\text{en})]$ the equilibrium constant defining the first aquation, pK_1 , decreased with increasing temperature. No similar trend was found for the second aquation equilibrium constant, pK_2 .

In contrast to 1,1/*t,t* ($n = 6$) where equilibrium conditions are achieved too rapidly to be measured by the collection of successive $[^1\text{H}, ^{15}\text{N}]$ HSQC NMR spectra,²⁴ the overall rate and extent of aquation of **1** permitted determination of reaction rates via this technique. Although a direct comparison of the rate constants obtained for **1** and 1,1/*t,t* ($n = 6$)²⁴ is not possible (the conditions used are not identical), it is evident from the data shown in Table 2 that the major difference in the aquation of the two species is in the magnitude of the aquation rate constant which is higher for 1,1/*t,t* ($n = 6$). A possible explanation is “nonproductive” ion-pairing between chloride ions and the central $\{\text{PtN}_4\}$ unit.

The aquation rate constant k_1 for **1** is approximately four times the value for the aquation rate constant of cisplatin under comparable conditions, in which the pH of the solution is 0.2–0.4 pH unit lower than the pK_a of the aquated platinum compound.¹⁴ The aquation rate constant from **2** to **1** is some 80-fold higher than the first aquation for cisplatin.¹⁴

(38) Miller, S. E.; House, D. A. *Inorg. Chim. Acta* **1989**, *161*, 131–137.

(39) Hindmarsh, K.; House, D. A.; Turnbull, M. M. *Inorg. Chim. Acta* **1997**, *257*, 11–18.

(40) Lee, K. W.; Martin, D. S. *Inorg. Chim. Acta* **1976**, *17*, 105–110.

(41) Reishus, J. W.; Martin, D. S. *J. Am. Chem. Soc.* **1961**, *83*, 2457–2462.

(42) Coley, R. F.; Martin, D. S. *Inorg. Chim. Acta* **1973**, *7*, 573–577.

The net result is that equilibrium conditions are established much more rapidly for **1** (2 h) than for cisplatin¹⁴ (ca 30 h) at 298 K in 0.01 M NaClO₄. The position of the equilibrium for **1**, like 1,1/t,t ($n = 6$),²⁴ favors the dichloro form to a much greater extent than does the aquation equilibrium of cisplatin at similar concentrations. The equilibrium constant (model 1, 298 K, $pK_1 = 3.44 \pm 0.04$) is also lower than for the other {PtClN₃} systems [PtCl(dien)]⁺ ($pK_1 = 3.9$ (293 K),⁴³ 3.7 (298 K)⁴⁴) and [PtCl(NH₃)₃]⁺ ($pK_1 = 4.1$ (293 K))⁴³ in which the extent of aquation is also limited by the relatively high chloride anation rate constants. Treatment of the aquation rate constant data from model 1 for **1** in 15 mM perchlorate at 288, 293, and 298 K to an Arrhenius analysis afforded an activation energy of 93 ± 3 kJ mol⁻¹. Applying the equilibrium constant using model 1 at 298 K afforded the following thermodynamic parameters for the aquation of **1** (in 15 mM NaClO₄): $\Delta G^\ddagger_{298K} = 96.2$ kJ mol⁻¹, $\Delta H^\ddagger_{298K} = 90.5$ kJ mol⁻¹, and $\Delta S^\ddagger_{298K} = -19.1$ J K⁻¹ mol⁻¹. The entropy value is consistent with an associative mechanism, as expected for square planar Pt(II).

The binding of phosphate to complexes with the {PtXN₃} moiety has been previously examined.^{45,46} Jacobs et al.⁴⁵ found that phosphate binding to [Pt(dien)(OH₂)]²⁺ was similar to that of chloride as seen by the similar values of the equilibrium constants for the conversion of [Pt(dien)(OH₂)]²⁺ to the phosphato ($pK = 2.81$) or chloro ($pK = 2.95$) complexes. A comparison of pK_1 and pK_3 values in Table 3 indicates that for **1** there is a clear preference for chloride over phosphate.

The binding of phosphate to **1** can be compared with a previous [¹H, ¹⁵N] HSQC NMR study of phosphate binding to cisplatin under similar conditions.¹⁴ In neither case does the presence of phosphate affect the initial aquation. There is no evidence for the formation of a phosphato species directly from *cis*-[PtCl(NH₃)₂(OH₂)]⁺, and it appears to be the diaqua species, *cis*-[Pt(NH₃)₂(OH₂)₂]²⁺, that binds phosphate. The first phosphate-bound species (*cis*-[Pt(OPO₃H₂)(NH₃)₂(OH/H)]) appears ca. 3 h after the start of the reaction.¹⁴ In contrast, for **1** a species with a bound phosphato ligand is observed within 15 min. This implies a kinetic preference in the binding of phosphate to the aquated form **2** relative to the mononuclear species. Thus, even though the equilibrium favors **1** over **2**, in the presence of phosphate, once formed **2** converts readily to **7**. At equilibrium there is a higher percentage of unreacted **1** in a solution of 15 mM phosphate than there is unreacted cisplatin under similar conditions. After 24 h reaction the concentration of cisplatin made up less than 25% of the total platinum concentration, while at equilibrium **1** accounted for 40% of the total. These differences may be a result of the higher anation rate constants found for **1**, keeping the overall equilibrium more

to the chloro form of the complex. Certainly, equilibrium conditions are established in the presence of phosphate far more rapidly for **1** than they are for cisplatin.¹⁴ Reversible binding of phosphate may have biological consequences. One of the major features of polynuclear compounds such as 1,1/t,t ($n = 6$) and BBR3464 is the enhanced cellular uptake of charged species:^{47,48} reversible reactions with negatively charged phosphates of amphiphilic anionic phospholipid membranes present an attractive postulate for a “shuttling” mechanism allowing uptake of these amphiphilic cations worthy of further exploration.

The pK_a value of the diaqua species, [{*trans*-Pt(¹⁵NH₃)₂(OH₂)₂}]₂{*μ-trans*-Pt{¹⁵NH₂(CH₂)₆¹⁵NH₂}₂(¹⁵NH₃)₂}]⁶⁺ (**3**), is the same as that found previously for 1,1/t,t ($n = 6$) (5.62).²⁴ As in the latter case it is reasonable to assume that the two {PtON₃} groups act independently so that the pK_a value for the coordinated water molecule in **2** should be similar to those of the diaqua species **3** and also the aquahydroxo species **5** (pK_{a2} and pK_{a3} , Scheme 2). For 1,1/t,t ($n = 6$) we speculated²⁴ that the inherent electrostatic repulsion of the end groups (a combination of charge and {Pt(NH₃)₂}-{Pt(NH₃)₂} repulsive interactions²⁴) should not be dramatically increased upon production of an aqua species so that it is unlikely that any difference in pK_a due to electrostatic factors would be measurable within the limits of the error. Electrostatic factors in the present case are even less likely given that for **3** the H₂O molecules coordinated to the two positively charged {PtN₃} groups are now separated by a total distance of ~25 Å and there is the central {PtN₄}²⁺ moiety which would tend to disrupt intermolecular association between dissolved molecules of **1**.

The pK_a of **2** (5.62) means that the major hydrolysis product of **1** will exist almost entirely in the less reactive hydroxo form (**4**) at physiological pH. On the basis of the calculated equilibrium and dissociation constants listed in Table 2 we calculate that, at physiological pH (7.2), the maximum tolerated dose of **1** in patients (1.8×10^{-8} M),³ and an intracellular Cl⁻ concentration of 22.7 mM (the recent value quoted by Jennerwein and Andrews⁴⁹ for A2008 human ovarian cancer cells), BBR3464 (**1**) will be 98.7% in the dichloro form at equilibrium. While this indicates that very little of **1** is hydrolyzed under these conditions, it still represents three times the concentration of hydrolyzed 1,1/t,t ($n = 6$) under equivalent conditions.²⁴ Of the hydrolyzed species from **1** (1.3% of the total) the OH/Cl form dominates **4**(96.1%):**2** (2.5%):**6**(1.3%):**5**(0.06%):**3**(0.0009%). In blood plasma, where the concentration of chloride is 103 mM,⁴⁹ only 0.3% of the total is aquated, but this increases slightly if the concentration of phosphate (~1.1 mM)^{50–52} is taken

(43) Marti, N.; Hoa, G. H. B.; Kozelka, J. *Inorg. Chem. Commun.* **1998**, 1, 439–442.

(44) Alcock, R. M.; Hartley, F. R.; Rogers, D. E. *J. Chem. Soc., Dalton Trans.* **1973**, 1070–1073.

(45) Jacobs, R.; Prinsloo, F.; Breet, E. *J. Chem. Soc., Chem. Commun.* **1992**, 212–213.

(46) Bose, R. N.; Gaoswami, N.; Maghaddas, S. *Inorg. Chem.* **1990**, 29, 3461–3467.

(47) Roberts, J. D.; Peroutka, J.; Farrell, N. *J. Inorg. Biochem.* **1999**, 77, 51–57.

(48) Roberts, J. D.; Peroutka, J.; Beggiolin, G.; Manzotti, C.; Piazzoni, L.; Farrell, N. *J. Inorg. Biochem.* **1999**, 77, 47–50.

(49) Jennerwein, M.; Andrews, P. A. *Drug Metab. Dispos.* **1995**, 23, 178–184.

(50) Drewes, P. A. *Clin. Chim. Acta* **1972**, 39, 81–88.

(51) Bosomworth, M. P.; Pearce, C. J. *Ann. Clin. Biochem.* **1989**, 26, 300–301.

(52) Yamamoto, T.; Moriwaki, Y.; Takahashi, S.; Tsutsumi, Z.; Yamakita, J.-I.; Higashino, K. *Metabolism* **1997**, 46, 1339–1342.

A Trinuclear Platinum Phase II Anticancer Agent

into consideration. Under these conditions, we calculate the speciation profile at equilibrium to be **1**(99.61%):**2**(0.30%):**7**(0.09%).

Acknowledgment. This work was supported by grants from the Australian Research Council, U.S. National Institutes of Health (RO1-CA78754), National Science Foundation (INT-9805552 and CHE-9615727), and The American Cancer Society (RPG89-002-11-CDD). We also thank Dr. Jim Fitzgerald for the preparation of $^{15}\text{NH}_2(\text{CH}_2)_6^{15}\text{NH}_2$.

Supporting Information Available: A table of the equilibrium and rate constants for the aquation of **1** according to a single aquation model (model 1). SCIENTIST models used to determine the rate constants given in Tables 2 and 3 for the aquation of **1** based on one aquation only and two aquation steps and in the presence of phosphate. Time dependence plots of species concentration for the aquation reactions in 15 mM ClO_4^- , pH 5.3 at 288 and 293 K, and in 100 mM at 298 K. This material is available free of charge via the Internet at <http://pubs.acs.org>.

IC010851N